Research Square

Preprints are preliminary reports that have not undergone peer review.
They should not be considered conclusive, used to inform clinical practice,
or referenced by the media as validated information.

CBCT–MRI–based prediction models for stratifying anterior disc displacement in orthodontic patients: development and independent internal validation of a retrospective diagnostic study

Ji-Teng Liu
The Affiliated Stomatological Hospital of Nanjing Medical University
Wei-Wen Fang
The Affiliated Stomatological Hospital of Nanjing Medical University
Xin-Yu Cai
The Affiliated Stomatological Hospital of Nanjing Medical University
Wei-Na Zhou
The Affiliated Stomatological Hospital of Nanjing Medical University
Si-Ze Li
State Key Laboratory Cultivation Base of Research, Prevention and Treatment for Oral Diseases
Zi-Jian Ban
State Key Laboratory Cultivation Base of Research, Prevention and Treatment for Oral Diseases
Guang-Rui Cao
State Key Laboratory Cultivation Base of Research, Prevention and Treatment for Oral Diseases
Yu-Li Wang
The Affiliated Stomatological Hospital of Nanjing Medical University
Zhang Yang
zyorth@njmu.edu.cn

The Affiliated Stomatological Hospital of Nanjing Medical University

Research Article

Keywords: Temporomandibular Joint Disorders, Cone-Beam Computed Tomography, Magnetic Resonance Imaging, Logistic Models, Decision Support Techniques

Posted Date: April 21st, 2026

DOI: https://doi.org/10.21203/rs.3.rs-9363437/v1

License: This work is licensed under a Creative Commons Attribution 4.0 International License.
Read Full License

Additional Declarations: No competing interests reported.

Version of Record: A version of this preprint was published at Oral Radiology on June 20th, 2026. See the published version at https://doi.org/10.1007/s11282-026-00947-1.

Abstract

Objectives

Undiagnosed anterior disc displacement (ADD) and anterior disc displacement without reduction (ADDwoR) during orthodontic treatment can compromise treatment outcomes and long-term stability. This study aimed to establish quantitative decision-support models for stratifying ADD and its subtypes based on the temporomandibular joint (TMJ) radiological morphology in order to address the diagnostic challenges in orthodontic patients with dentofacial deformities.

Methods

In this retrospective diagnostic study, 72 patients (144 TMJs) awaiting orthodontic treatment were allocated to a modeling group (n = 61) and an independent internal validation group (n = 11), with TMJ imaging indicators (joint space, disc thickness, condylar dimensions, and condylar volume) quantified using CBCT and MRI. TMJs were stratified into normal, anterior disc displacement with reduction (ADDwR), or ADDwoR groups according to MRI disc-condylar angle. Diagnostic models were developed using Spearman's correlation analysis, logistic regression, and were visualized as nomograms, with internal validation via the Bootstrap method and independent internal validation using the validation group. Model reliability was evaluated using the intraclass correlation coefficient (ICC), goodness-of-fit tests, and McNemar tests, while discriminative ability was assessed via receiver operating characteristic (ROC) curve analysis.

Results

Two logistic regression models were developed. The ADD diagnosis model (AUC = 0.925) included anterior joint space, posterior band thickness, and condylar diameters (APCD and MLCD); the ADDwoR subclassification model (AUC = 0.898) incorporated anterior band thickness, middle band thickness, and condylar volume. Optimized thresholds (0.629, 0.748) had sensitivities (75.8%, 90.6%), specificities (87.1%, 78.2%), and good consistent calibration curves ($P > 0.05$), with no validation group-reference differences ($P = 0.063, 0.125$).

Conclusions

The developed logistic regression models could be explored as a potential imaging-based tool for ADD subtyping, offering supplementary information in orthodontic clinical decision-making for ambiguous TMD cases and potentially aiding treatment planning in orthodontic and craniofacial practice.

Introduction

Temporomandibular disorder (TMD), particularly anterior disc displacement (ADD), represents a significant and multifaceted challenge in contemporary orthodontic practice [1, 2]. Their impact compromises treatment outcomes: diagnostic accuracy, biomechanical feasibility, and long-term stability [3–5]. Clinically, symptoms such as joint pain, muscle tenderness, and restricted mandibular mobility often obscure the patient's true physiological mandibular position and occlusal relationship, which has direct consequences across the treatment process. Restricted mobility impedes the accurate assessment of the functional balance of the jaw-masticatory muscle system (the coordination between mandibular spatial position, condyle-disc-fossa structural matching, and masticatory muscle function) during diagnosis, which can lead to an incorrect evaluation of treatment needs [6]. As a general principle, active orthodontic treatment should be suspended upon the onset of temporomandibular joint (TMJ) pain and may only be resumed following adequate symptomatic improvement [2]. If the underlying dysfunction remains unaddressed, it may also induce compensatory occlusal adaptations that threaten long-term stability and increase the risk of relapse. Applying conventional orthodontic forces to an unstable or dysfunctional masticatory system is not only biomechanically inefficient but may also exacerbate existing symptoms, provoke further joint adaptation, or contribute to iatrogenic damage [6, 7].

The clinical management and risk profile in orthodontic patients are critically determined by the specific subtype of ADD present [8]. The essential distinction lies between anterior disc displacement with reduction (ADDwR) and without reduction (ADDwoR), defined by the disc's ability to recapture onto the condylar head during opening [9]. ADDwoR, characterized by a permanently displaced disc and often accompanied by progressive soft tissue remodeling, is associated with a higher propensity for chronic pain, accelerated joint degeneration, and significant functional impairment [4]. Initiating comprehensive orthodontic treatment without prior recognition and appropriate management of underlying ADDwoR substantially increases the risk of therapeutic complications, including exacerbated pain, compromised mechanics, and ultimately, treatment failure or relapse [1, 2]. Therefore, differentiating ADDwR from ADDwoR through precise pretreatment diagnostic stratification of TMD is beneficial and imperative. It forms the essential basis for risk assessment, informed patient consent, and the development of a staged, interdisciplinary treatment approach that prioritizes joint stabilization as a prerequisite for definitive orthodontic care.

Currently, the diagnosis of ADD relies primarily on a combination of clinical examinations and imaging modalities, particularly the MRI and CBCT, constituting critical diagnostic tools for the assessment and subclassification of ADD in TMD [6, 8]. MRI of the TMJ is a highly effective diagnostic imaging modality that provides comprehensive and high-resolution anatomical details, such as disc morphology, disc positioning, disc thickness and condylar structure, making it indispensable for distinguishing between ADD subtypes [6–10]. Complementarily, CBCT is increasingly used in orthodontic practice for 3D assessment of dentofacial structures and provides detailed, cross-sectional imaging of the osseous structures, thereby enabling precise identification of skeletal abnormalities and joint deformities and facilitating the indirect inference of potential disc displacement within the TMJ [8–10]. While MRI is unequivocally established as the gold standard for visualizing disc position and stratifying ADD [6–10],

diagnostic challenges persist in borderline cases. In such scenarios, where the disc-condyle relationship is not unequivocally pathological or when differentiating between ADDwR and ADDwoR is difficult based on visual assessment alone, inter-observer variability may increase. Moreover, visual assessment alone may not fully capture the spectrum of morphological alterations, such as precise disc thickness variations and condylar bone remodeling, that are associated with disease severity and progression from reducible to irreducible stages [11–13].

To address these gaps, quantifying the morphological features of the TMJ using imaging data has emerged as a promising decision support aid. Previous observations suggest that quantitative parameters derived from MRI (e.g., disc thickness) and CBCT (e.g., joint space, condylar diameter, condylar volume) may correlate significantly with the presence and subtype of ADD [11–14]. Integrating these parameters into a data-driven decision-support model, such as logistic regression, could help address the limitations of traditional methods and assist in clinical diagnosis [15].

Based on the imaging data and regression model techniques, this study investigates the correlation between the radiological morphology of the TMJ and the diagnosis of ADD in orthodontic patients with dentofacial deformities. By utilizing the quantitative parameters of TMJ morphology, an evaluation model for the diagnosis of ADD was developed and validated, aiming to provide orthodontists with a quantitative framework to objectively identify and subclassify ADD, thereby facilitating more informed, personalized, and biologically sound treatment decisions.

Materials and methods

Collection of research subjects

This retrospective diagnostic study included 72 patients (144 TMJs) awaiting orthodontic treatment with confirmed dentofacial deformities, who underwent bilateral TMJ CBCT and MRI at Nanjing Medical University Affiliated Stomatological Hospital (November 2022 - December 2023). The cohort comprised 20 males (40 TMJs) and 52 females (104 TMJs), aged 8–75 years (mean 25.71 ± 14.62 years). All included patients had atypical TMD clinical symptoms, inconsistent physical signs and preliminary imaging findings, and could not be clearly classified into ADD subtypes through routine oral examination. The participants were randomly divided into two groups: the model establishment group (n = 61, 18 males and 43 females) and the model validation group (n = 11, 2 males and 9 females).

Sample size calculation was performed referring to the method of Sui et al. [16], with assumptions of a model AUC of 0.8, $\alpha = 0.05$ and power = 0.8, confirming that the sample size of 144 TMJs was sufficient to ensure the statistical validity of model construction and independent internal validation. Moreover, given that an events per variable (EPV) of 10 is conventionally deemed sufficient for model stability, we adopted a more stringent threshold of EPV > 20 in the present analysis. This methodological decision specifically accounts for the clustering effect inherent to bilateral temporomandibular joint data obtained from the same patient, thereby further mitigating the potential for model overfitting.

Inclusion and exclusion criteria

The DC/TMD (Diagnostic Criteria for Temporomandibular Disorder) standardized protocol and diagnostic taxonomy are widely regarded as critical and essential tools in clinical research on TMD, and are recognized for their methodological rigor and relevance in enhancing diagnostic accuracy [4].

Inclusion criteria:

1. Adults/adolescents with clinical symptoms of TMD;
2. Temporomandibular joint ADD confirmed by MRI examination on at least one side;
3. Time interval between the TMJ CBCT and MRI examinations not exceeding 3 months;
4. Confirmed dentofacial deformity or occlusal abnormalities requiring orthodontic treatment.
5. Patients with atypical TMD clinical symptoms, inconsistent physical signs and preliminary imaging findings, and cannot be clearly classified into ADD subtypes through routine clinical examination.

Exclusion Criteria:

1. Non-TMD orofacial pain conditions;
2. History of active systemic diseases or structural anomalies or trauma;
3. Inability to complete protocol.

MRI imaging

MRI images of the bilateral TMJs were obtained at both closed and wide-open mouth positions using the same Siemens 3.0 T superconducting MRI machine. In the closed-mouth position, patients maintained the maximum intercuspal position with the Frankfurt horizontal (FH) plane aligned parallel to the ground. In the open-mouth position, patients opened maximally (about 35mm or more) with a calibrated bite block. Oblique sagittal and oblique coronal images were obtained in both positions. The oblique sagittal scan plane was oriented to visualize the long axis of the condyle and the oblique coronal scan plane was perpendicular to the long axis of the condyle. Three pulse sequences (T1WI, T2WI, PDWI) were executed for scanning and detailed scanning parameters are provided in Table S1. Slices per sequence were dynamically set to 12–18 (slice thickness: 2 mm, slice gap: 0.2 mm) to fully cover the condylar mediolateral dimension.

Upon completion of the scanning procedure, the MRI images were recorded in Digital Imaging and Communications in Medicine (DICOM) format. A total of 144 lateral TMJ images from 72 participants were collected, including oblique sagittal T1WI, T2WI, and PDWI sequences for both the open and closed mouth positions.

CBCT imaging

CBCT images were obtained utilizing a NewTom 5G CT system (QR srl, Verona, Italy) to ensure optimal spatial resolution for unilateral TMJ coverage. Detailed scanning parameters are provided in Table S2. Participants were positioned in the maximum intercuspal position for closed-mouth scans and instructed to open utilizing a calibrated bite block for open-mouth scans, with the midsagittal plane perpendicular to the horizontal plane and the FH plane aligned parallel to the ground through laser-guided verification.

The CBCT software was utilized for the reconstruction and processing of TMJ images, wherein standardized multiplanar reorientation was initiated by identifying the transverse ridge of the condyle on the axial view to define the condylar long axis as a line connecting the medial and lateral poles, with verification in the coronal plane. Based on this established axis, oblique sagittal images were generated parallel to the condylar orientation, while oblique coronal images were reconstructed perpendicular to the defined condylar axis. All CBCT imaging data were archived in DICOM format, ensuring methodological reproducibility.

Experimental grouping

In clinical practice, the position of the articular disc is commonly described utilizing the disc-condyle angle. According to Drace's diagnostic criteria [17], in the MRI closed oblique sagittal view, a clear demarcation line exists between the posterior band of the articular disc and the bilaminar zone, referred to as the disc-condyle line. The angle formed between this line and the 12-point plumb line drawn along the condylar eminence is known as the disc-condyle angle. A disc-condyle angle ranging from − 15° to 15° in the anteroposterior direction indicates a normal disc-condyle relationship (Fig. 1A), when the disc is observed between the 11:30 and 12:30 clock positions on MRI scans [18, 19]. An angle greater than 15° anteriorly suggests an anterior displacement of the disc (Fig. 1B), while an angle greater than 15° posteriorly indicates a posterior displacement of the disc [17, 20, 21].

The 144 lateral joints were categorized into two primary groups based on the size of the disc-condyle angle: ADD and no anterior disc displacement (Table 1, Part 1), and the ADD was further classified into two subcategories: ADDwR and ADDwoR, according to whether the disc returned to its normal position during jaw opening (Table 1, Part 2). All analyses and classifications in this study were performed on a per-joint basis. The status of each TMJ (ADD or Normal) was determined independently, regardless of the contralateral joint's condition.

Table 1
Distribution of TMJ diagnostic categories in the modeling and validation cohorts Part 1 Distribution of joints with and without anterior disc displacement (ADD and normal)

Disc displacement type	Disc-condyle angle (°)	Number of TMJs	
		Model establishment group	Model validation group
ADD	≥ 16°	91	19
Normal	−15° to 15°	31	3
Total		122	22

Part 2 Distribution of joints with anterior disc displacement with reduction (ADDwR) and without reduction (ADDwoR)

ADD subgroup types	Definition (Disc reduction during mouth opening)	Number of TMJs	
		Model establishment group	Model validation group
ADDwoR	Disc is not reduced to normal position	53	10
ADDwR	Disc is reduced to normal position	38	9
Total		91	19

Measurement of TMJ imaging morphological parameters

Disc thickness

The oblique sagittal plane exhibiting the articular disc's maximal cross-sectional area was selected for morphometric analysis which was identified through multiplanar reconstruction centered on the condylar transverse ridge, with three critical dimensional parameters: the maximal thickness quantification of both anterior and posterior disc bands, along with the minimal thickness measurement of the intermediate band [22] (Fig. 2A).

Measurement of CBCT imaging morphological parameters

Joint space

Joint space measurements were performed according to the Kamelchuk [23] protocol. Two parallel horizontal reference lines (L1, L2) were established along the FH plane, with L1 tangent to the articular fossa's superior surface and L2 tangent to the condylar head's superior border. The vertical distance between these lines was recorded as the supra-articular dimension (S). Additional reference lines (L3,

L4) were constructed as tangents to the condyle's anterior and posterior margins, originating from the superior articular fossa's tangent point. Perpendicular projections from these lines were then established through the respective condylar margin tangent points to determine the anterior (A) and posterior (P) joint space parameters (Fig. 2B).

Condylar anteroposterior and transverse diameters

The closed-mouth CBCT image displaying the maximum cross-sectional area of the condyle was selected for dimensional analysis, with measurements performed along two orthogonal axes: the mediolateral diameter representing the condylar long axis measured as the linear distance between the innermost [M] and outermost [L] points of the condyle, parallel to the condylar movement trajectory, and the anteroposterior diameter corresponding to the short axis determined by constructing a perpendicular through the midpoint [O] of ML to intersect the most anterior [A] and posterior [P] condylar margins, with the AP distance calculated as the linear measurement between these terminal points (Fig. 2C).

Condyle volume

The CBCT data in DICOM format was imported into Mimics 21.0 software (Materialise, Leuven, Belgium) for 3D reconstruction of condyle. The condylar boundary was delineated utilizing standardized grayscale thresholds (226–3071 Hounsfield Units), with the initial horizontally appearing high-density structure identified as the condylar apex, while the first image demonstrating complete separation between the articular eminence and condyle served as the condylar base [24, 25]. Three-dimensional reconstruction was performed with limited manual contour refinement only on ambiguous boundaries utilizing Multiplanar Edit tools across sagittal, coronal, and axial planes. The preliminary 3D rendering underwent refinement through smoothing algorithms (smoothing coefficient = 3) and surface wrapping procedures, with final boundary definition achieved via Contour Editing protocols to generate the definitive anatomical model which corresponded to the volume of the condyle (Fig. 2D).

To ensure objectivity and minimize inter-observer variability, all assessments were performed independently by two investigators within the same month.

Statistical analysis

Data analysis was performed with SPSS Statistics (version 27.0; IBM Corporation) and R software (version 4.2.2). This study was designed, implemented, and reported with reference to the TRIPOD statement (Transparent Reporting of a multivariable prediction model for Individual Prognosis Or Diagnosis), to standardize the reporting process and improve the transparency and methodological quality of the clinical prediction models.

1. Measurement Reliability Assessment:

All imaging parameters included in the model were entered into the logistic regression model as original continuous values without dichotomization or classification, thereby maximizing the retention of original

data information and avoiding information loss caused by artificial grouping. On this basis, the measurement reliability of all TMJ morphological parameters was further evaluated.

Measurement reliability of all TMJ morphological parameters was evaluated using intraclass correlation coefficients (ICC). Duplicate assessments were independently conducted by two investigators within one month to minimize inter-observer variability. An ICC value > 0.9 was defined as excellent reproducibility, confirming the consistency of measurement methods.

2. Descriptive Statistics and Intergroup Comparisons:

Continuous variables were expressed as median values with interquartile ranges (IQR). Nonparametric statistical methods were applied for intergroup comparisons: the Mann-Whitney U test was used to compare parameter differences between the ADD group and the normal group, as well as between the ADDwoR group and the ADDwR subgroup.

3. Correlation Analysis:

Spearman’s rank correlation coefficients were used to explore bivariate associations between radiographic parameters (e.g., anterior joint space, posterior band thickness, condylar volume) and clinical diagnostic outcomes (presence of ADD, subtype of ADDwoR), which identified potential predictive factors for subsequent model construction.

4. Model Construction:

Two binary logistic regression models were separately developed using data from the model establishment group to address distinct diagnostic objectives: The primary model was developed to predict the presence of ADD, and the secondary model was developed to subclassify ADD into ADDwR and ADDwoR.

The forward stepwise selection was employed for variable screening, with the inclusion criterion set at $\alpha = 0.05$ and the exclusion criterion set at $\alpha = 0.10$, which continued until no additional variables satisfied the predefined inclusion criterion.

5. Model Validation and Evaluation:

The final models were presented as nomograms for clinical use and underwent comprehensive validation:

1. Internal Statistical Properties: Multicollinearity among predictors was assessed using variance inflation factors (VIFs), with a value exceeding 10 indicating concern. The overall significance of the model coefficients was verified by likelihood ratio tests.

(2) Model Discrimination: The model's ability to distinguish between outcomes was evaluated using receiver operating characteristic (ROC) curve analysis. The area under the curve (AUC) was calculated,

and the optimal diagnostic threshold was determined by maximizing the Youden index. Corresponding sensitivity and specificity, along with their 95% confidence intervals, were reported.

(3) Calibration and Goodness-of-Fit: The agreement between predicted probabilities and observed outcomes was appraised. Calibration plots were generated for both the establishment and validation cohorts, with bootstrap resampling (100 iterations) applied to correct for overfitting. Additionally, the Hosmer–Lemeshow test was used to assess model fit statistically.

(4) Independent internal Validation: The generalizability of the models was tested by applying them to an independent validation cohort (11 patients, 22 TMJs). The concordance between model-predicted classifications and the reference standard diagnoses was evaluated using the McNemar test.

In this retrospective diagnostic study, 72 patients (144 TMJs) awaiting orthodontic treatment were divided into a modeling group and an independent internal validation group. TMJ imaging parameters (joint space, disc thickness, condylar dimensions, and volume) were quantified via CBCT and MRI (detailed scanning parameters in Table S1 and Table S2), and TMJs were stratified into normal, ADDwR, and ADDwoR groups based on the MRI disc-condylar angle. Two logistic regression models for ADD diagnosis and ADDwoR subclassification were developed and validated using statistical analyses. For the detailed study workflow, refer to Fig. S1.

Results

Parameter Analysis

All TMJ parameters demonstrated excellent measurement reliability (ICC = 0.977–0.999), indicating outstanding measurement reproducibility. The study comprised 91 ADD cases (74.59%) and 31 controls (25.41%). Significant between-group variations were identified in the anterior and superior joint space, anterior, middle and posterior disc bands, APCD, MLCD, and the condylar volume, all demonstrating significant associations with ADD status, while posterior joint space dimensions exhibited neither significant group differences nor clinical associations (Table 2, Part 1). Subgroup analysis revealed 38 cases of ADDwR (41.76%) and 53 cases of ADDwoR (58.24%) among the ADD group. Significant between-group differences were observed in posterior joint space, anterior, middle, and posterior articular disc thicknesses and the condylar volume. However, no significant associations were found regarding the anterior and superior joint space, or APCD and MLCD (Table 2, Part 2).

Table 2

Imaging features of the temporomandibular joint: **comparison between diagnostic groups Part 1 Comparison of Radiographic Parameters Between the ADD Group and the Normal Group**

Parameter	ADD Group (n = 91) Median (IQR)	Normal Group (n = 31) Median (IQR)	Z	P	r
Anterior joint space (mm)	2.300 (1.610–2.890)	1.650 (1.370-2.000)	3.546	< 0.001***	0.322
Superior joint space (mm)	2.395 (1.940–2.905)	2.865 (2.730–3.270)	−3.567	< 0.001***	−0.324
Posterior joint space (mm)	1.945 (1.440–2.640)	2.075 (1.785–2.605)	−0.876	0.381	−0.080
Thickness of anterior band (mm)	2.350 (1.960–2.975)	3.220 (2.345–3.545)	−3.061	0.002**	−0.278
Thickness of middle band (mm)	0.960 (0.825–1.240)	0.770 (0.680–1.060)	2.729	0.006**	0.248
Thickness of posterior band (mm)	2.155 (1.750–2.730)	3.375 (2.635–4.095)	−5.111	< 0.001***	−0.465
APCD (mm)	5.100 (4.300–6.080)	7.605 (6.015–9.055)	−5.213	< 0.001***	−0.474
MLCD (mm)	14.685 (11.905–17.385)	18.295 (16.515–20.210)	−4.966	< 0.001***	−0.451
Condylar volume (mm^3)	1588.500 (1055.670-1856.135)	1781.475 (1478.845-2164.280)	−2.802	0.005**	−0.255
*p < 0.05, **p < 0.01, ***p < 0.001					

Abbreviations: APCD, anteroposterior condylar diameter; MLCD, mediolateral condylar diameter

Part 2 Comparison of Radiographic Parameters Between the ADDwoR Group and the ADDwR Group

Parameter	ADDwoR Group (n = 53) Median (IQR)	ADDwR Group (n = 38) Median (IQR)	Z	P	r
Anterior joint space (mm)	2.390 (1.628-2.888)	2.115 (1.594-2.905)	0.676	0.499	0.071
Superior joint space (mm)	2.395 (2.003-2.983)	2.403 (1.860-2.805)	0.563	0.573	0.059
Posterior joint space (mm)	2.090 (1.735-2.993)	1.720 (1.201-2.169)	2.942	0.003**	0.310
Thickness of anterior band (mm)	2.220 (1.815-2.533)	3.005 (2.225-3.809)	−3.919	<0.001***	−0.413
Thickness of middle band (mm)	1.130 (0.923-1.383)	0.833 (0.633-1.011)	4.415	<0.001***	0.465
Thickness of posterior band (mm)	1.995 (1.663-2.618)	2.455 (1.885-3.109)	−2.298	0.022*	−0.242
APCD (mm)	5.045 (4.313-5.680)	5.233 (4.059-7.100)	−0.575	0.565	−0.061
MLCD (mm)	13.805 (11.890-17.260)	14.750 (11.996-17.673)	−0.857	0.391	−0.090
Condylar volume (mm^3)	1234.130 (959.625-1729.193)	1728.885 (1370.621-2057.550)	−3.460	<0.001***	−0.365

*p < 0.05, **p < 0.01, ***p < 0.001

Abbreviations: APCD, anteroposterior condylar diameter; MLCD, mediolateral condylar diameter

Model establishment

Through the forward stepwise selection, the regression frameworks for ADD and ADDwoR converged to optimized predictor sets. The finalized ADD decision-support model incorporated four statistically significant morphometric determinants (α = 0.05), while the ADDwoR classification model retained three validated predictors collectively establishing the diagnostic algorithms (Table 3, Part 1 and 2).The established disease assessment models are expressed in Equations (1) and (2), where P_{ADD} denotes the

diagnostic probability of ADD in the ADD model, and P_{ADDwoR} represents the diagnostic probability of ADDwoR in the ADDwoR model.

Testing of models

Variance inflation factor (VIF) values below 10 confirmed the absence of significant multicollinearity among the independent variables in both models. Nomograms were constructed based on the two final logistic regression models to visualize the predictive probability of ADD and ADDwoR (Fig. 3A and B), and the corresponding calibration curves showed good consistency between predicted probabilities and actual clinical outcomes (Fig. 3C and D). Both developed models satisfied all established validation criteria, including likelihood ratio test requirements ($p < 0.05$), qualitative model fit evaluations through residual analysis, and quantitative goodness-of-fit metrics (Table 3, Part 3). The imaging data of the validation group were used to compare the diagnostic results of the two models with the actual diagnoses. The McNemar test showed that there was no significant difference between the diagnostic results of the regression model and the standard diagnosis (ADD: P = 0.063, ADDwoR: P = 0.125), suggesting preliminary consistency of the models. However, limited by the small sample size of the validation cohort, the reliability and generalizability of the models still need to be further verified in larger multi-center cohorts. ROC analysis demonstrated that the ADD model exhibited an AUC of 0.925 (95% CI: 0.878-0.971), while the ADDwoR model achieved a higher discriminative ability with an AUC of 0.898 (95% CI: 0.827-0.968), with optimal diagnostic thresholds identified at 0.629 (sensitivity 75.8%, specificity 87.1%) and 0.748 (sensitivity 90.6%, specificity 78.2%), respectively, based on Youden index (Fig. 3E).

Table 3 Multivariable logistic regression models for ADD and ADDwoR

Part 1 Multivariate binary logistic regression analysis of the ADD group and the Normal group

Predictors and intercept	B	SE	Wald χ^2	P	OR	95% CI
Intercept	8.117	2.070	15.371	< 0.001	3351.056	——
Anterior joint space (mm)	1.107	0.497	4.969	0.026*	3.025	[1.143-8.007]
Thickness of posterior band (mm)	−1.162	0.359	10.481	0.001**	0.313	[−0.1455 to −0.632]
APCD (mm)	−0.358	0.166	4.648	0.031*	0.699	[−0.505 to −0.968]
MLCD (mm)	−0.227	0.104	4.746	0.029*	0.797	[−0.650 to −0.977]

*p < 0.05, **p < 0.01, ***p < 0.001

Abbreviations: APCD, anteroposterior condylar diameter; MLCD, mediolateral condylar diameter

Part 2 Multivariate binary logistic regression analysis of the ADDwR group and the ADDwoR group

Predictors and intercept	B	SE	Wald χ^2	P	OR	95% CI
Intercept	2.784	1.668	2.788	0.095	16.186	——
Thickness of anterior band	−1.650	0.527	9.805	0.002**	0.192	[−0.068 to −0.539]
Thickness of middle band	4.663	1.271	13.450	< 0.001***	105.915	[8.765-1279.855]
Volume of condyle	−0.002	0.001	8.184	0.004**	0.998	[−0.997 to −0.999]

*p < 0.05, **p < 0.01, ***p < 0.001

Part 3 Goodness-of-fit indicators for the ADD and ADDwoR decision-support models

Model	Likelihood ratio test	-2 Log likelihood	Nagelkerke R^2	Hosmer-Lemeshow test
ADD Model	χ^2 =63.061 P < 0.001***	75.236	0.404	P = 0.264
ADDwoR Model	χ^2 =53.718 P < 0.001***	69.951	0.600	P = 0.234

*p < 0.05, **p < 0.01, ***p < 0.001

1. $$\text{Logit(PADD)} = 8.117 + 1.107 \times [\text{Anterior joint space (mm)}] - 1.162 \times [\text{Posterior band thickness (mm)}] - 0.358 \times [\text{APCD (mm)}] - 0.227 \times [\text{MLCD (mm)}]$$

2. $$\text{Logit(PADDwoR)} = 2.784 - 1.650 \times [\text{Anterior band thickness (mm)}] + 4.663 \times [\text{Middle band thickness (mm)}] - 0.002 \times [\text{Condylar volume } (\text{mm}^3)]$$

Discussion

The integration of TMD assessment, specifically for subtyping ADD and ADDwoR, into the orthodontic diagnostic workflow is important for clinically stable treatment plans [26]. However, in clinically ambiguous or borderline cases, even experienced orthodontists may face challenges in accurately stratifying ADD through subjective evaluation methods, such as observing mandibular movement during mouth opening and closing or interpreting disc-condyle positional relationships on MRI [1]. Previous studies have confirmed the significant correlation between quantitative imaging parameters of CBCT/MRI and the occurrence of ADD, but most of them focused on patients with pure temporomandibular disorders, and there are relatively limited studies on developing stratified diagnostic

prediction models for ADD in orthodontic patients with dentofacial deformities [27]. Unlike previous studies based on pure TMD specialist samples, this study focused on patients awaiting orthodontic treatment with dentofacial deformities, which may better represent the actual clinical scenario of orthodontists. The findings aim to providea quantitative reference framework for orthodontists to systematically evaluate TMJ status before operation, thereby contributing to the existing evidence for the combination of TMD diagnosis and orthodontic treatment planning.

The decision-support model identifies several cardinal physiological markers reflecting TMJ degeneration, which may suggest implications for orthodontic assessment. (1) Disc morphology changes: Posterior band thinning (OR = 0.313, P = 0.001) in the ADD model suggests increased TMJ vulnerability to abnormal biomechanical loading, suggesting potentially a treatment plan favoring light, continuous forces (e.g., low-intensity traction, passive alignment techniques) and avoiding aggressive mandibular advancement should be prioritized [28, 29]. And middle band thickening (OR = 105.915, P < 0.001) in the ADDwoR model strongly indicates its role as a robust predictor for differentiating ADDwoR from ADDwR, which results from prolonged mechanical stress during irreversible displacement, serving as a prognostic indicator for surgical necessity—thicker middle bands often correlate with poorer response to conservative treatments due to reduced disc elasticity [10, 29, 31]. It suggests that the patient's path to a stable occlusion may require an altered treatment sequence. (2) Condylar volume reduction (OR = 0.998, P = 0.004) is a key marker of TMJ bone remodeling induced by chronic joint stress, which implies that orthodontic treatment should abandon aggressive skeletal correction goals and prioritize dental compensation instead [32]. Meanwhile, long-term retention strategies must be strengthened. Using fixed retainers instead of removable appliances, extending retention duration to 2–3 years to maintain the achieved occlusal relationship and prevent further condylar resorption or joint damage are worth considering [33, 34]. (3) Anterior joint space widening (OR = 3.025, P = 0.026) reflects the biomechanical alterations associated with anterior disc displacement, accompanied by tensile failure of the bilaminar zone [35]. Conventional Class II traction (e.g., intermaxillary elastics from maxillary molars to mandibular canines) should be avoided because its posterior force will further push the condyle into the already crowded posterior structure, which is likely to exacerbate discomfort, pain, and even irritating inflammation in the joint region and accelerate condylar resorption [8, 36]. Alternative approaches, such as temporary anchorage devices (TADs) for distalization of maxillary molars or intrusion of anterior teeth, are preferred to minimize joint loading [37].

In recent years, artificial intelligence (AI) methods have been widely integrated with clinical diagnosis. Contemporary research has validated the diagnostic efficacy of deep learning architectures in this domain. As evidenced by Lee et al. [38], a deep convolutional neural network (CNN) framework achieved superior specificity compared to clinical specialists in detecting disc displacement abnormalities through MRI analysis. This study screened and verified the key quantitative imaging markers associated with ADD and its subtypes, which can provide a reference for feature selection in the subsequent development of artificial intelligence-assisted automatic diagnosis model for TMJ ADD.

It should be emphasized that this study does not advocate for exclusive reliance on AI models for ADD diagnosis; rather, for patients with clinically indicated imaging data, the proposed model serves as an effective decision support tool for medical practitioners [39]. Measuring parameters such as disc thickness still requires the ability to identify anatomical structures on MRI. Therefore, the primary utility of this model lies in providing an objective, quantitative framework to support decision-making for orthodontists, particularly in borderline cases or for less experienced practitioners. It serves as a complementary tool that quantifies key morphological changes associated with ADD.

Several constraints should be acknowledged in the interpretation of these findings. Primarily, the generalizability of our models may be constrained by the relatively modest sample size and the single-center, homogenous nature of the participant cohort, and further verification in multi-ethnic populations is needed to expand the independent internal validity of these findings. Secondly, the predictive accuracy of the models could potentially be enhanced by the integration of key clinical variables, such as age and symptom duration, which were not included in the current imaging-centric analysis. Thirdly, this study adopted a joint-level analysis that assumed the left and right temporomandibular joints of the same patient were independent of each other, which may have underestimated the within-subject correlation and affected the accuracy of model inference [40]. Future research with larger, prospectively recruited multi-center cohorts, stringent bilaterally normal control groups, and integrated clinical data is imperative to translate these quantitative imaging biomarkers into the more robust clinical tools.

In conclusion, this study establishes reliable quantitative imaging biomarkers for ADD diagnosis utilizing a combination of CBCT and MRI parameters. The identified morphological changes in joint spaces, articular discs, and condyles provide objective criteria for clinical assessment, while the developed decision-support models offer a data-driven approach to enhance diagnostic precision and inform personalized therapeutic strategies in orthodontic and craniofacial practice.

Conclusion

This retrospective single-center diagnostic study developed and validated two quantitative decision-support models based on integrated CBCT and MRI imaging parameters for the auxiliary stratification of ADD and its subtypes in orthodontic patients with dentofacial deformities. The ADD diagnosis model (AUC = 0.925) and the ADDwoR subclassification model (AUC = 0.898) demonstrated robust diagnostic performance, highlighting the clinical utility of key morphological parameters such as joint space dimensions, disc thickness, and condylar volume. These models establish a reproducible, imaging-based framework that shows potential to enhance diagnostic accuracy, particularly in clinically ambiguous cases, and could supports orthodontists in making biologically informed decisions. By integrating quantitative imaging biomarkers into routine orthodontic assessment, this approach has the potential to facilitate personalized treatment planning, improve risk stratification, and contribute to the long-term stability of craniofacial and occlusal outcomes. Future multi-center studies incorporating clinical variables and larger cohorts are warranted to further refine and generalize these models.

Declarations

TRIPOD STATEMENT

This study was designed, implemented, and reported in accordance with the TRIPOD statement (Transparent Reporting of a multivariable prediction model for Individual Prognosis Or Diagnosis) to ensure the quality and credibility of the clinical prediction models established in this research.

FUNDING

This study was supported by the Jiangsu Provincial Health Commission General Project (No. M2024053) and Jiangsu College Student's Innovative and Entrepreneurial Capability Program (No. X2025103120189).

Author Contribution

Ji-Teng Liu: Conceptualization, Formal analysis, Visualization, Methodology, and Writing – original draft; Wei-Wen Fang: Conceptualization, Investigation, Methodology, and Project administration; Xin-Yu Cai: Funding acquisition, Data curation, and Formal analysis; Wei-Na Zhou: Resources, Methodology, and Project administration; Si-Ze Li: Formal analysis, and Investigation; Zi-Jian Ban: Formal analysis, and Investigation; Guang-Rui Cao: Conceptualization and Investigation; Yu-Li Wang: Project administration, Supervision, and Writing – review & editing; Yang Zhang: Conceptualization, Funding acquisition, Project administration, Supervision, and Writing – review & editing. All authors commented on previous versions of the manuscript. All authors have read and approved the final version of the manuscript.

Data Availability

The data can be accessed on reasonable request to the corresponding author.

References

1. Ehrmann E, Bernabeu M, Tillier Y, et al. Impact of Orthodontic-Surgical Treatments on the Signs and Symptoms of Temporomandibular Disorders: A Systematic Review. Dent J (Basel). 2024;12(5):132. 10.3390/dj12050132. Published 2024 May 8.
2. Alam MK, Abutayyem H, Alzabni KMD, et al. The Impact of Temporomandibular Disorders on Orthodontic Management: A Systematic Review and Meta-Analysis. Cureus. 2023;15(8):e44243. 10.7759/cureus.44243. Published 2023 Aug 28.
3. Sergl HG, Klages U, Zentner A. Pain and discomfort during orthodontic treatment: causative factors and effects on compliance. Am J Orthod Dentofac Orthop. 1998;114(6):684–91. 10.1016/s0889-

5406(98)70201-x.

4. Schiffman E, Ohrbach R, Truelove E, et al. Diagnostic Criteria for Temporomandibular Disorders (DC/TMD) for Clinical and Research Applications: recommendations of the International RDC/TMD Consortium Network* and Orofacial Pain Special Interest Group†. J Oral Facial Pain Headache. 2014;28(1):6–27. 10.11607/jop.1151.
5. Wolford LM. Can orthodontic relapse be blamed on the temporomandibular joint? J Orthod Sci. 2014;3(4):95–105. 10.4103/2278-0203.143227.
6. Luther F. Orthodontics and the temporomandibular joint: where are we now? Part 1. Orthodontic treatment and temporomandibular disorders. Angle Orthod. 1998;68(4):295–304. 10.1043/0003-3219(1998)068%3C0295:OATTJW%3E2.3.CO;2.
7. Zhang R, Lai D, Zhang F, et al. A Comparative Analysis of Temporomandibular Disorders Using a Jaw Motion Analyzer and Surface Electromyography. Int Dent J. 2025;75(3):1843–53. 10.1016/j.identj.2025.03.023.
8. Liu W, Wu Z, Hu Y, et al. Temporomandibular Disorders in Adolescents and Adults With Different Disc-Condyle Relationships: A Longitudinal Comparative Study. J Oral Rehabil Published online September. 2025;26. 10.1111/joor.70066.
9. Talmaceanu D, Lenghel LM, Bolog N, et al. Imaging modalities for temporomandibular joint disorders: an update. Clujul Med. 2018;91(3):280–7. 10.15386/cjmed-970.
10. Fan PD, Xiong X, Cheng QY, et al. Risk estimation of degenerative joint disease in temporomandibular disorder patients with different types of sagittal and coronal disc displacements: MRI and CBCT analysis. J Oral Rehabil. 2023;50(1):12–23. 10.1111/joor.13385.
11. Liu SS, Xu LL, Lu SJ, Mao MY, Liu LK, Cai B. Diagnostic performance of magnetic resonance imaging for degenerative temporomandibular joint disease. J Oral Rehabil. 2023;50(1):24–30. 10.1111/joor.13386.
12. Yu W, Jeon HH, Kim S, Dayo A, Mupparapu M, Boucher NS. Correlation between TMJ Space Alteration and Disc Displacement: A Retrospective CBCT and MRI Study. Diagnostics (Basel). 2023;14(1):44. 10.3390/diagnostics14010044. Published 2023 Dec 25.
13. Mohamed HN, Ashmawy MS, Ekladious MEY, Farid MM. Analysis of the relationship between condylar changes and anterior disc displacement with reduction: a preliminary study. Oral Radiol. 2023;39(1):154–63. 10.1007/s11282-022-00617-y.
14. Gao Y, Luo D, Yuan M, Yang Y, Xu Z, Yang J. The relationship between the oblique sagittal temporomandibular joint disc position and the volume surface area of the condyle in young TMD adults. Front Bioeng Biotechnol. 2023;11:1321241. 10.3389/fbioe.2023.1321241. Published 2023 Dec 21.
15. Emshoff R, Bertram A, Hupp L, Rudisch A. A logistic analysis prediction model of TMJ condylar erosion in patients with TMJ arthralgia. BMC Oral Health. 2021;21(1):374. Published 2021 Jul 24. 10.1186/s12903-021-01687-w

16. Sui H, Xiao M, Jiang X, Li J, Qiao F, Yin B, Wang Y, Wu L. Development and validation of a predictive nomogram for bilateral posterior condylar displacement using cone-beam computed tomography and machine-learning algorithms: a retrospective observational study. BMC Oral Health. 2025;25(1):916. 10.1186/s12903-025-06098-9IF: 3.1 Q1. PMID: 40474172; PMCID: PMC12142821.
17. Drace JE, Enzmann DR. Defining the normal temporomandibular joint: closed-, partially open-, and open-mouth MR imaging of asymptomatic subjects. Radiology. 1990;177(1):67–71. 10.1148/radiology.177.1.2399340.
18. Ahmad M, Hollender L, Anderson Q, et al. Research diagnostic criteria for temporomandibular disorders (RDC/TMD): development of image analysis criteria and examiner reliability for image analysis. Oral Surg Oral Med Oral Pathol Oral Radiol Endod. 2009;107(6):844–60. 10.1016/j.tripleo.2009.02.023.
19. Taşkaya-Yilmaz N, Oğütcen-Toller M, Saraç YS. Relationship between the TMJ disc and condyle position on MRI and occlusal contacts on lateral excursions in TMD patients. J Oral Rehabil. 2004;31(8):754–8. 10.1111/j.1365-2842.2004.01309.x.
20. Lei J, Yap AU, Li Y, Liu MQ, Fu KY. Clinical protocol for managing acute disc displacement without reduction: a magnetic resonance imaging evaluation. Int J Oral Maxillofac Surg. 2020;49(3):361–8. 10.1016/j.ijom.2019.07.005.
21. Fu KY, Hu M, Yu Q, et al. Zhonghua Kou Qiang Yi Xue Za Zhi. 2020;55(9):608–12. 10.3760/cma.j.cn112144-20200514-00268.
22. Wang M, Cao H, Ge Y, Widmalm SE. Magnetic resonance imaging on TMJ disc thickness in TMD patients: a pilot study. J Prosthet Dent. 2009;102(2):89–93. 10.1016/S0022-3913(09)60116-5.
23. Kamelchuk LS, Grace MG, Major PW. Post-imaging temporomandibular joint space analysis. Cranio. 1996;14(1):23–9. 10.1080/08869634.1996.11745945.
24. Schlueter B, Kim KB, Oliver D, Sortiropoulos G. Cone beam computed tomography 3D reconstruction of the mandibular condyle. Angle Orthod. 2008;78(5):880–8. 10.2319/072007-339.1.
25. Tecco S, Saccucci M, Nucera R, et al. Condylar volume and surface in Caucasian young adult subjects. BMC Med Imaging. 2010;10:28. 10.1186/1471-2342-10-28. Published 2010 Dec 31.
26. Klur T, Portegys S, Graf I, Scharf S, Braumann B, Kruse T. Temporomandibular Disorders: Management of Diagnostics and Therapy in the Context of Orthodontic Treatment-A Survey Among German Orthodontists. Dent J (Basel). 2025;13(4):167. 10.3390/dj13040167. Published 2025 Apr 17.
27. Lin B, Cheng M, Wang S, Li F, Zhou Q. Automatic detection of anteriorly displaced temporomandibular joint discs on magnetic resonance images using a deep learning algorithm. Dentomaxillofac Radiol. 2022;51(3):20210341. 10.1259/dmfr.20210341.
28. Zhao M, Wang P, Wang H, Li X, Bai D, Tian Y. Diagnostic and treatment protocol for a patient with temporomandibular disorder using a stabilization splint and temporary anchorage devices. Am J Orthod Dentofac Orthop. 2021;159(5):666–e6812. 10.1016/j.ajodo.2020.05.015.

29. Demirovic K, Dzemidzic V, Nakas E. Impact of Stabilization Splint Therapy on Orthodontic Diagnosis in Patients with Signs and Symptoms of Temporomandibular Disorder. Biomedicines. 2024;12(10):2251. Published 2024 Oct 3. 10.3390/biomedicines12102251
30. Wang XD, Cui SJ, Liu Y, et al. Deterioration of mechanical properties of discs in chronically inflamed TMJ. J Dent Res. 2014;93(11):1170–6. 10.1177/0022034514552825.
31. Yildirim D, Dergin G, Tamam C, Moroglu S, Gurses B. Indirect measurement of the temporomandibular joint disc elasticity with magnetic resonance imaging. Dentomaxillofac Radiol. 2011;40(7):422–8. 10.1259/dmfr/98030980.
32. Xiao X, Cheng Y, Zou S, Chen J. Computer-aided surgical workflow in a surgery - First orthognathic approach to correct anterior open bite in a young adult with temporomandibular disorders. Int Orthod. 2022;20(1):100600. 10.1016/j.ortho.2021.10.007.
33. Guo D, Zhou Z, Sun K, et al. Fully digital workflow of occlusal reconstruction treatment in a patient with congenital dentition defects. J Esthet Restor Dent. 2024;36(9):1236–48. 10.1111/jerd.13234.
34. Cheng X, Haotian Y, Zhu X. Orthodontic reconstruction of the jaw in the treatment with TMD. Int Dent J. 2025;75:105554. 10.1016/j.identj.2025.105554.
35. Imanimoghaddam M, Madani AS, Mahdavi P, Bagherpour A, Darijani M, Ebrahimnejad H. Evaluation of condylar positions in patients with temporomandibular disorders: A cone-beam computed tomographic study. Imaging Sci Dent. 2016;46(2):127–31. 10.5624/isd.2016.46.2.127.
36. Gurbanov V, Bas B, Öz AA. Evaluation of Stresses on Temporomandibular Joint in the Use of Class II and III Orthodontic Elastics: A Three-Dimensional Finite Element Study. J Oral Maxillofac Surg. 2020;78(5):705–16. 10.1016/j.joms.2019.11.022.
37. Hsu LF, Liu YJ, Wang SH, Chen YJ, Chen YJ, Yao CJ. Orthodontic correction of acquired open bite with TMJ degeneration: A retrospective study of outcomes and stability. J Formos Med Assoc. 2024;123(4):452–60. 10.1016/j.jfma.2023.10.006.
38. Lee YH, Won JH, Kim S, Auh QS, Noh YK. Advantages of deep learning with convolutional neural network in detecting disc displacement of the temporomandibular joint in magnetic resonance imaging. Sci Rep. 2022;12(1):11352. Published 2022 Jul 5. 10.1038/s41598-022-15231-5
39. Duyan Yüksel H, Orhan K, Evlice B, Kaya Ö. Evaluation of temporomandibular joint disc displacement with MRI-based radiomics analysis. Dentomaxillofac Radiol. 2025;54(1):19–27. 10.1093/dmfr/twae066.
40. Kakimoto N, Wongratwanich P, Shimamoto H et al. Comparison of T2 values of the displaced unilateral disc and retrodiscal tissue of temporomandibular joints and their implications. Sci Rep. 2024;14(1):1705. Published 2024 Jan 19. 10.1038/s41598-024-52092-6

Figures

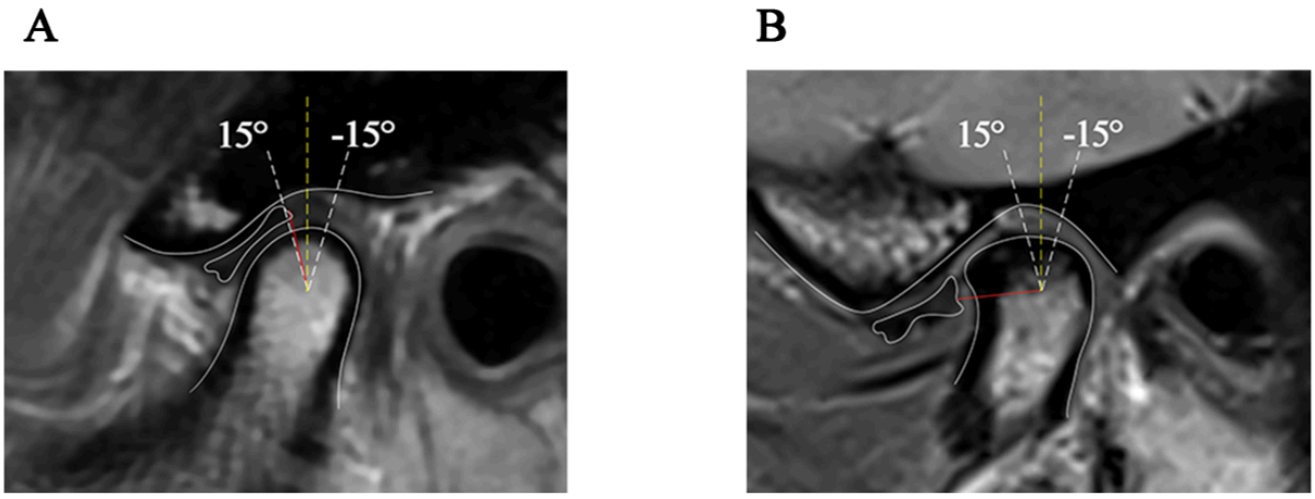


Figure 1

Schematic diagram of MRI-based disc displacement classification (A) Normal disc position (disc-condyle angle between −15° and 15°); (B) **Anterior disc displacement (**ADD; disc-condyle angle > 15°)

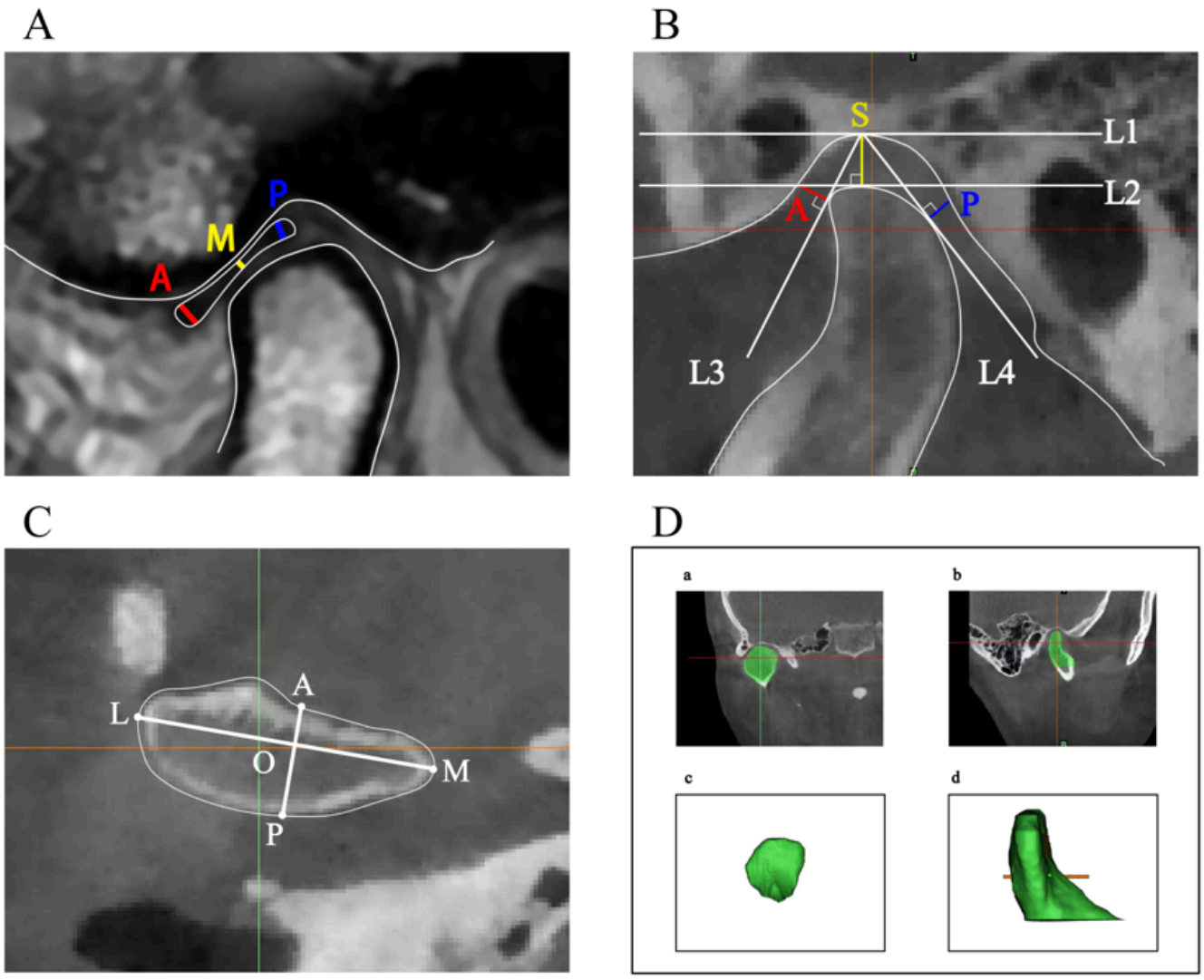


Figure 2

Quantitative measurements of TMJ morphology on MRI and CBCT (A) Three reference lines used to measure disc thickness: **A**, anterior band thickness; **M**, intermediate band thickness; **P**, posterior band thickness. (B) Kamelchuk's method for measuring CBCT joint space dimensions (superior, anterior, and posterior joint spaces). (C) Measurement of condylar diameters on CBCT: ML span, mediolateral condylar diameter (long axis); AP span, anteroposterior diameter (short axis), measured perpendicular to ML at its midpoint. (D) Three-dimensional reconstruction of the condyle from CBCT data: (a) coronal view of the condyle; (b) sagittal view of the condyle; (c) coronal view of the 3D model; (d) sagittal view of the 3D model

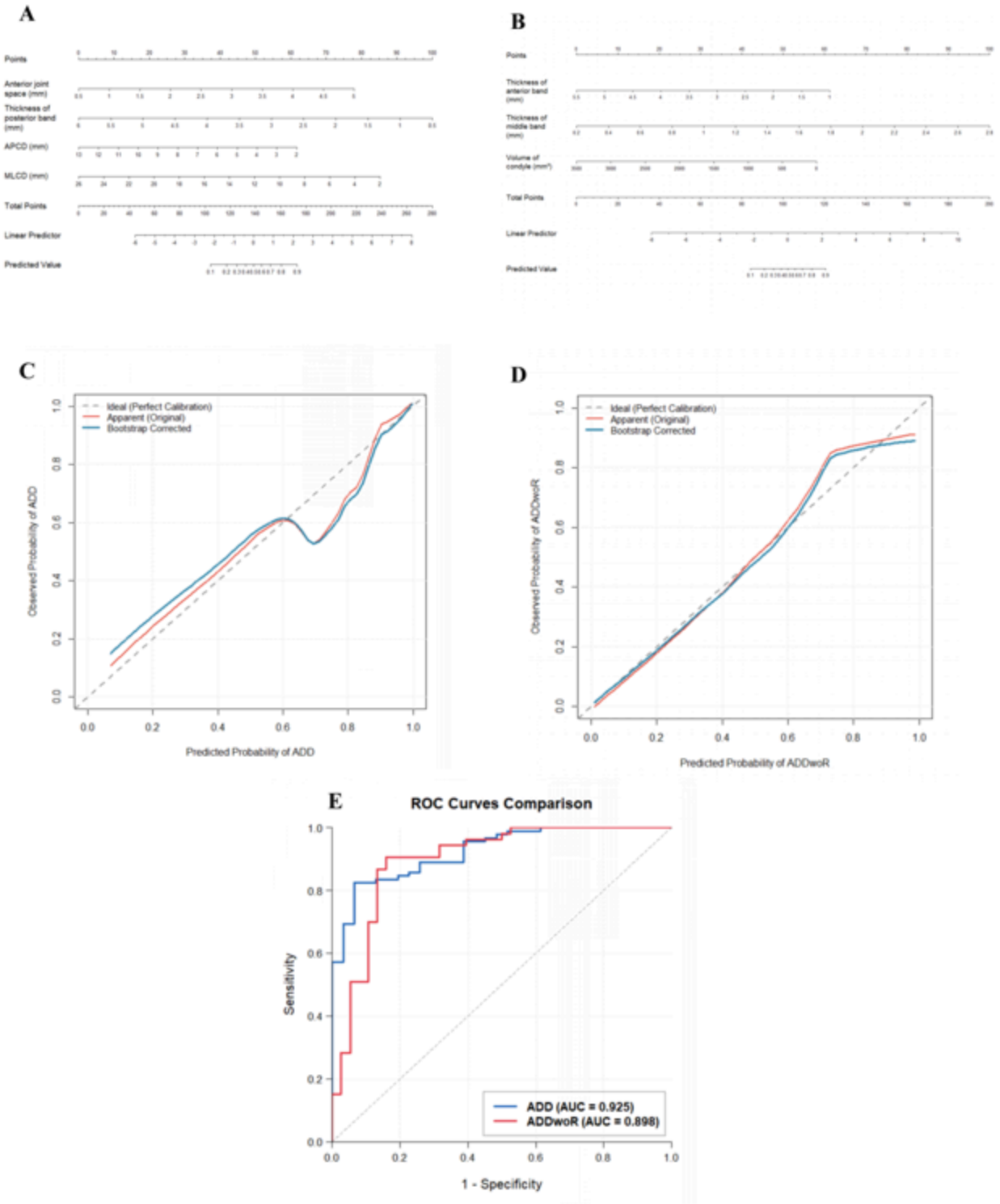


Figure 3

Decision-support models for ADD and ADDwoR (A) Nomogram of the ADD decision-support model in patients with dentofacial deformities; (B) Nomogram of the ADDwoR decision-support model in patients with dentofacial deformities; (C) Calibration curve of the ADD model in the modeling cohort, showing agreement between predicted and observed probabilities after bootstrap resampling (100 iterations); (D) Calibration curve of the ADDwoR model in the modeling cohort, showing agreement between predicted

and observed probabilities after bootstrap resampling (100 iterations); (E) ROC curves of the ADD and ADDwoR decision-support models in the modeling cohort (AUC = 0.925 and 0.898, respectively)

Supplementary Files

This is a list of supplementary files associated with this preprint. Click to download.

- SuppInfo.docx